

**DISCOVERING THE HIGGS BOSONS
OF MINIMAL SUPERSYMMETRY WITH MUONS**

CHUNG KAO¹

*Department of Physics and Astronomy, University of Rochester
Rochester, NY 14627, USA*

NIKITA STEPANOV²

*Institute of Theoretical and Experimental Physics
Moscow, Russia*

Abstract

The prospects of detecting neutral Higgs bosons in the minimal supersymmetric model via their decays into muon pairs at the LHC are investigated. The CMS detector performance is adopted for a realistic study of observability. It is found that the muon pair decay mode might provide a very promising channel to search for the neutral Higgs bosons of minimal supersymmetry. This channel will allow precise mass reconstruction for neutral Higgs bosons.

¹Internet Address: KAO@URHEP.PAS.ROCHESTER.EDU

²Internet Address: STEPANOV@CERNVM.CERN.CH

1 Introduction

One of the most important experimental goals of future hadron supercolliders such as the CERN Large Hadron Collider (LHC) is to unravel the mystery of electroweak symmetry breaking, to produce and to detect the Higgs bosons or to prove their non-existence. In the Standard Model (SM) of electroweak interactions, only one Higgs doublet is required to generate masses for fermions as well as gauge bosons. One neutral CP-even Higgs boson (H^0) appears after spontaneous symmetry breaking. Various extensions of the SM have more complicated Higgs sectors and lead to additional physical spin zero fields [1].

The minimal supersymmetric extension of the Standard Model (MSSM) [2] has two Higgs doublets with vacuum expectation values v_1 and v_2 . After spontaneous symmetry breaking, there remain five physical Higgs bosons: a pair of singly charged Higgs bosons H^\pm , two neutral CP-even scalars H (heavier) and h (lighter), and a neutral CP-odd pseudoscalar A . The Higgs sector is strongly constrained by supersymmetry so that at the tree level, all Higgs boson masses and couplings are determined by just two independent parameters, which are commonly chosen to be the mass of the CP-odd pseudoscalar (M_A) and $\tan \beta \equiv v_2/v_1$.

Since the top quark is very heavy [3, 4], radiative corrections from large t -quark Yukawa couplings substantially modify the tree level formulae for masses and mixing patterns in the Higgs sector. Several groups have reevaluated prospects for the detection of MSSM Higgs bosons at future hadron colliders. Most studies have focused on various SM decay modes for the neutral Higgs bosons, $\phi \rightarrow \gamma\gamma$ and $\phi \rightarrow ZZ$ or $ZZ^* \rightarrow 4l$ ($\phi = H, h$ and A); as well as for the charged Higgs boson [5], that are detectable above background. Parameters were selected such that supersymmetric particle (SUSY particle) masses were large so that Higgs boson decays to SUSY particles were kinematically forbidden [6]-[10]. A region of parameter space roughly spanning pseudoscalar Higgs mass $M_A \sim 100 - 300$ GeV and ratio

of Higgs VEV's $\tan\beta \sim 4 - 10$ where none of the SM decay modes were detectable. For large $\tan\beta$, the $\tau\bar{\tau}$ decay mode [10, 11, 12] has been suggested to be a promising discovery channel. Recently, it has been argued that neutral Higgs bosons might be observable via their $b\bar{b}$ decays [13, 14, 15] in a large region of the $(M_A, \tan\beta)$ plane, provided that sufficient b -tagging capability can be achieved. Signals for invisible decays of Higgs bosons have also been considered [16]-[21]. In addition, there are regions of parameter space where rates for Higgs boson decays to SUSY particles are large and dominant. While these decays reduce the rates for SM signatures, making conventional detection of Higgs bosons even more difficult, they also open up a number of new promising modes for Higgs detection [22].

In this paper, the prospects of discovering the neutral Higgs bosons in the MSSM via their decays into muon pairs³ at the LHC are investigated. Parton level calculations are presented in Section II. The CMS detector performance is adopted for a realistic study of observability. Results from realistic simulations are discussed in Section 3 and promising conclusions are drawn in Section 4.

2 Parton Level Calculations

In our analysis, the cross section of $pp \rightarrow \phi \rightarrow \mu\bar{\mu} + X$ is evaluated from the Higgs boson cross section $\sigma(pp \rightarrow \phi + X)$ multiplied with the branching fraction of the Higgs decay into muon pairs $B(\phi \rightarrow \mu\bar{\mu})$. The parton distribution functions of CTEQ2L [23] are chosen to evaluate the cross section of $pp \rightarrow \phi + X$ with $\Lambda_4 = 0.190$ GeV and $Q^2 = M_\phi^2 + P_T^2$, where P_T is the transverse momentum of the Higgs bosons. We take $M_Z = 91.187$ GeV, $\sin^2\theta_W = 0.2319$, $M_W = M_Z \cos\theta_W$, $m_b = 4.7$ GeV, and $m_t = 175$ GeV. We have included one loop corrections from top and bottom Yukawa interactions to the Higgs masses and couplings using the effective potential [24]-[26] with $A_t = A_b = 0$. The contributions from

³This discovery channel may not be useful to search for the SM Higgs boson [1].

the D-terms are usually small [22], therefore, they are not included. We consider two sets of parameters similar to those discussed in Ref. [22], (a) $m_{\tilde{g}} = m_{\tilde{q}} = \mu = 1000$ GeV, such that the Higgs boson decays to SUSY particles are kinematically forbidden; and (b) $m_{\tilde{g}} = m_{\tilde{q}} = \mu = 300$ GeV, such that the Higgs boson decays to SUSY particles are large and dominant when $\tan\beta$ is less than about 10. The K-Factors are not included for the signal or the background.

At the LHC energy, the SM Higgs boson (H^0) is produced dominantly from gluon fusion [27], and from vector boson fusion [28]-[30] if the Higgs boson is heavy. In the MSSM, gluon fusion ($gg \rightarrow \phi$) is the major source of neutral Higgs bosons for $\tan\beta$ less than about 4. If $\tan\beta$ is larger than about 10, neutral Higgs bosons in the MSSM are dominantly produced from b -quark fusion ($b\bar{b} \rightarrow \phi$) [31]. We have evaluated the cross section of Higgs bosons in pp collisions $\sigma(pp \rightarrow \phi + X)$, with two dominant subprocesses: $gg \rightarrow \phi$ and $gg \rightarrow \phi b\bar{b}$. The cross section of $gg \rightarrow \phi b\bar{b}$ is a good approximation to the ‘exact’ cross section [31] of $b\bar{b} \rightarrow \phi$ for M_ϕ less than about 500 GeV. In addition, the subprocesses $gg \rightarrow \phi b\bar{b}$ and $gg \rightarrow g\phi$ are complementary to each other for producing large P_T Higgs bosons at future hadron colliders [32, 33, 34]. Since the Yukawa couplings of $\phi b\bar{b}$ are enhanced by $1/\cos\beta$, the production rate of neutral Higgs bosons is usually enhanced with large $\tan\beta$. For M_A larger than about 150 GeV, the couplings of the lighter scalar h to gauge bosons and fermions become close to those of the SM Higgs boson, therefore, gluon fusion is the major source of the h even if $\tan\beta$ is large.

If the $b\bar{b}$ mode dominates Higgs decays, the branching fraction of $\phi \rightarrow \mu\bar{\mu}$ is about $(m_\mu/m_b)^2$. It has been found that QCD radiative corrections reduce the decay width of $\phi \rightarrow b\bar{b}$ by a factor of about 2 [35, 36]. Therefore, the branching fraction of $\phi \rightarrow \mu\bar{\mu}$ is about 2×10^{-4} when the $b\bar{b}$ mode dominates. Let’s consider a parameter space of $(M_A, \tan\beta)$ with $50 \text{ GeV} \leq M_A \leq 500 \text{ GeV}$ and $1 \leq \tan\beta \leq 35$. The branching fraction of $B(h \rightarrow \mu\bar{\mu})$ in the whole parameter space as well as $B(A \rightarrow \mu\bar{\mu})$ and $B(H \rightarrow \mu\bar{\mu})$ with $\tan\beta \gtrsim 10$ is

always about 2×10^{-4} , even when A and H can decay into SUSY particles. For M_A less than about 80 GeV, the H decays dominantly into hh , AA and ZA .

Fig. 1 shows the cross section of $pp \rightarrow \phi \rightarrow \mu\bar{\mu} + X$ as a function of M_A for various values of $\tan\beta$. We have taken $m_{\tilde{q}} = \mu = 1$ TeV. For $\tan\beta \gtrsim 10$, the production cross section is always enhanced. As expected, the cross section of $pp \rightarrow h \rightarrow \mu\bar{\mu} + X$ does not change much with $\tan\beta$ for $M_A > 150$ GeV. Also shown is the same cross section for the SM Higgs boson H^0 with $M_{H^0} = M_A$. For $M_{H^0} > 140$ GeV, the SM H^0 mainly decays into gauge bosons, therefore, the branching fraction $B(H^0 \rightarrow \mu\bar{\mu})$ drops sharply.

We define the signal to be observable if the 99% confidence level upper limit on the background is smaller than the corresponding lower limit on the signal plus background [6, 37], namely,

$$\begin{aligned} L(\sigma_s + \sigma_b) - N\sqrt{L(\sigma_s + \sigma_b)} &> L\sigma_b + N\sqrt{L\sigma_b} \\ \sigma_s &> \frac{N^2}{L}[1 + 2\sqrt{L\sigma_b}/N] \end{aligned} \quad (1)$$

where L is the integrated luminosity, and σ_b is the background cross section within a bin of width $\pm\Delta M_{\mu\bar{\mu}}$ centered at M_ϕ ; $N = 2.32$ corresponds to a 99% confidence level and $N = 2.5$ corresponds to a 5σ signal.

To study the observability of the muon discovery mode, we consider the background from the Drell-Yan (DY) process, $q\bar{q} \rightarrow Z, \gamma \rightarrow \mu\bar{\mu}$, which is the dominant background. We take $\Delta M_{\mu\bar{\mu}}$ to be the larger of the CMS muon mass resolution or the Higgs boson width. The minimal cuts applied are (1) $p_T(\mu) > 10$ GeV and (2) $|\eta(\mu)| < 2.5$, for both the signal and background. More details about the background will be discussed in next section.

The 5σ discovery contours at $\sqrt{s} = 14$ TeV are shown in Fig. 2, for (a) $L = 100$ fb $^{-1}$, $\mu = m_{\tilde{q}} = 1000$ GeV, (b) $L = 100$ fb $^{-1}$, $\mu = m_{\tilde{q}} = 300$ GeV, and (c) $L = 10$ fb $^{-1}$, $\mu = m_{\tilde{q}} = 1000$ GeV. The A might be detectable in a large region of parameter space with $\tan\beta$ away from one. The H might be observable in a region with $M_A > 120$ GeV and

$\tan\beta \gtrsim 10$. The h might be observable in a region with $M_A < 120$ GeV and $\tan\beta \gtrsim 4$. This channel is affected by the SUSY decay modes only slightly for H and h [38]. The lighter top squarks will make the H and h lighter and enhance the $Hb\bar{b}$ coupling while reducing the $hb\bar{b}$ coupling. Therefore, the discovery region of $H \rightarrow \mu\bar{\mu}$ is slightly enlarged for a smaller M_A , but the observable region of $h \rightarrow \mu\bar{\mu}$ is slightly reduced.

3 Realistic Simulations

Like the $\gamma\gamma$ mode, the discovery potential of the $\mu\mu$ channel is very sensitive to the detector performance. Therefore, one needs to fix some detector model for quantitative estimates. The CMS detector performance parameters are used in our analysis to estimate the signal and backgrounds. The CMS will be one of two general purpose LHC detectors, and the very precise muon momentum reconstruction is one of its main parameters, which define the detector design [12]. Thus, it will be an excellent detector to look for the narrow di-muon resonances.

3.1 Calculation tools

We use PYTHIA 5.7 and JETSET 7.4 generators [39] with the CTEQ2L [23] parton distribution functions to simulate events on the particle level. In the case of DY background near the Z -peak, QED corrections are very important and have been taken into account by treating the $Z \rightarrow \mu\bar{\mu}$ decay with the computer program PHOTOS [40].

In addition to $gg \rightarrow \phi$, the new debugged PYTHIA [41] allows one to use $gg \rightarrow \phi b\bar{b}$ process for the production of all neutral MSSM Higgs bosons. The generated kinematics and total cross sections are in reasonable agreement with analytical parton level calculations. For our purpose we adapted in PYTHIA the program calculating 1-loop corrected masses and couplings [42]. The PYTHIA/JETSET/PHOTOS outputs are processed with the CMSJET program [43]. It is developed for fast simulations of "realistic" CMS detector

response. The resolution effects are taken into account by using the parametrizations obtained from the detailed GEANT [44] simulations. CMSJET includes also some analysis programs, in particular, a set of jet reconstruction algorithms, etc.

For future analysis, all muons with transverse momentum $p_T(\mu) \geq 5$ GeV and pseudorapidity $|\eta(\mu)| \leq 2.4$; missing transverse momentum \cancel{p}_T ; central jets with transverse energy $E_T \geq 40$ GeV and $|\eta| \leq 2.4$ are reconstructed and stored for each generated event.

3.2 Backgrounds and optimal kinematical cuts

There are several SM physical processes that generate sizeable muon pairs⁴. However, analyzing them process by process, one can conclude, that there is only one dominant subprocess in the interesting mass range ($50 \text{ GeV} \leq M_{\mu\bar{\mu}} \leq 500 \text{ GeV}$), which is the DY muon pair production [45]. For low $M_{\mu\bar{\mu}} \lesssim 100$ GeV the $b\bar{b}$ background is also potentially dangerous, but it can be reduced easily well below the DY process with isolation cuts on muons. The background from top quark pairs ($t\bar{t}$) is negligible in the region $|M_{\mu\bar{\mu}} - M_Z| \leq 30$ GeV. It is about 20 times smaller than the DY for $M_{\mu\bar{\mu}} \lesssim 150$ GeV and begins to compete with the DY for the highest $M_{\mu\bar{\mu}}$. About 90% of muon pairs in $t\bar{t}$ production are generated from the decay chain $t\bar{t} \rightarrow WWb\bar{b} \rightarrow \mu\bar{\nu}\bar{\mu}\nu b\bar{b}$. For comparison, the event rate from WW is 3-5 times lower than that from $t\bar{t}$.

To optimize the kinematical cuts, sizeable ($\sim 10^6$) background event samples are generated using the production chain described above. Our analysis indicates, that, in fact, after $M_{\mu\bar{\mu}}$ is constrained in a small bin around some fixed M_ϕ (we are looking for the narrow states), there are no further suitable kinematical cuts to suppress the dominant DY background. So here some minimal cuts, providing good signal efficiency and acceptance are used: $p_T(\mu) \geq 10$ GeV with $|\eta(\mu)| \leq 2.4$. The $t\bar{t}$ background can be reduced nearly by

⁴SUSY backgrounds from the lightest chargino pairs and from the second lightest neutralino decays are currently under investigation. In our analysis, we assume that they could be reduced significantly with a cut on missing transverse energy, similar to the $t\bar{t}$ decays.

a factor of 5 with additional cuts: missing transverse energy $E_T \leq 50$ GeV, $N_{jet} \leq 1$ for jets with $E_T \geq 40$ GeV, and $|\eta(jet)| \leq 2.4$. The muon isolation reduces the $b\bar{b}$ background by a factor of about 100.

3.3 Results

The invariant mass distribution ($d\sigma/dM_{\mu\bar{\mu}}$) of the backgrounds from (a) Drell-Yan, (b) W^+W^- , (c) $t\bar{t}$, and (d) $b\bar{b}$, are shown in Fig. 3.

Fig. 4 shows the 5σ significance contour for CMS detector and $L = 100$ fb $^{-1}$ with minimal cuts discussed above and isolation criteria applied for low masses ($M_{\mu\bar{\mu}} \leq 85$ GeV). In this figure, we have considered the total cross section of $pp \rightarrow \phi \rightarrow \mu\mu + X$, summed over the h , the H and the A . For $M_A \lesssim 200$ GeV and $\tan\beta \geq 25 - 30$, an integrated luminosity of 10 fb $^{-1}$ would be sufficient to obtain Higgs signals with a statistical significance larger than 7. But in the region close to the Z - peak, the signal is marginal despite the large significance, because it appears on the shoulder of the huge Z - peak. Only an adequate subtraction procedure, if it would be possible, enables one to extract the signal in this region.

Despite the high di-muon mass resolution of CMS detector (about 0.5% for $M_{\mu\bar{\mu}} \simeq 100$ GeV and better than 2% for $M_{\mu\bar{\mu}} \lesssim 500$ GeV), for large $\tan\beta \sim 30$ one can obtain the unresolved (h,A) signal for $M_A \lesssim 120$ GeV or (H,A) signal for higher M_A , because the mass difference between the (h,A) or (H,A) Higgs bosons is several hundreds MeV, i.e. a factor of 10 less than Higgs widths. Only for the lowest accessible $\tan\beta \sim 10 - 15$ it seems to be possible to resolve the signals for two resonances. But the signal become not so significant. Fig. 5 illustrates the signal over the backgrounds as function of $M_{\mu\bar{\mu}}$ at $\sqrt{s} = 14$ TeV with an integrated luminosity of 100 fb $^{-1}$, $M_A = 80, 150$ GeV, and $\tan\beta = 30$. This figure is generated from a simulation with the CMS performance and $m_{\tilde{q}} = \mu = 1000$ GeV.

4 Conclusions

It is found that the muon pair decay mode can be a very promising channel to discover the neutral Higgs bosons of minimal supersymmetry. The discovery region of the $\mu\bar{\mu}$ might be slightly smaller than the $\tau\tau$ channel but it will allow precise reconstruction for the Higgs boson masses. The A might be observable in a large region of parameter space with $\tan\beta$ away from one. The H might be detectable in a large region with $M_A > 120$ GeV and $\tan\beta \gtrsim 10$. The h might be observable in a region with $M_A < 120$ GeV and $\tan\beta \gtrsim 4$.

For $M_A \leq 200$ GeV and $\tan\beta > 25$, $L = 10 \text{ fb}^{-1}$ would be enough to obtain Higgs boson signals with a statistical significance larger than 7. For $M_{\mu\bar{\mu}}$ close to the M_Z , the signal is marginal despite the large significance, because it appears on the shoulder of the huge Z peak. Adequate subtraction procedures are required to extract the signal in this region. One attractive possibility is to tag the b -jets accompanying the $\mu\bar{\mu}$ from the Higgs decay, since the production rate of Higgs bosons via $gg \rightarrow \phi b\bar{b}$ is large. With high b -tagging efficiency and purity, we can reduce the dominant DY background to the level of $Z + b\bar{b}$ production. In this case, the $t\bar{t}$ background may become dangerous, and the additional cuts discussed above may be crucial. This signature is currently under study.

Acknowledgements

We would like to thank Howie Baer and Xerxes Tata for beneficial discussions and comments, and especially, Duane Dicus for continuing encouragement as well as instructions. This research was supported in part by the US Department of Energy grant DE-FG02-91ER40685.

References

- [1] J. Gunion, H. Haber, G. Kane and S. Dawson, *The Higgs Hunter's Guide*, (Addison-Wesley Publishing Company, Redwood City, CA, 1990).
- [2] Reviews for the MSSM can be found in: H.P. Nilles, Phys. Rep. **110**, (1984) 1; P. Nath, R. Arnowitt and A. Chamseddine, *Applied N = 1 Supergravity*, ICTP Series in Theoretical Physics, Vol.I, World Scientific (1984); H. Haber and G. Kane, Phys. Rep. **117**, (1985) 75; X. Tata, in *The Standard Model and Beyond*, edited by J. E. Kim, World Scientific (1991).
- [3] F. Abe *et al.*, Phys. Rev. Lett. **73** (1994) 225; Phys. Rev. **D50** (1994) 2966; F. Abe *et al.*, the CDF Collaboration, FERMILAB-PUB-95-022-E.
- [4] S. Abachi *et al.*, Phys. Rev. Lett. **72** (1994) 2138; S. Abachi *et al.*, the D0 Collaboration, FERMILAB-PUB-95-028-E.
- [5] Recent studies on the search for charged Higgs boson in the MSSM are to be found in: Felcini, in *Proceedings of the Large Hadron Collider Workshop*, Aachen (1990), p. 414, Vol. II, CERN 90-10; D.P. Roy, Phys. Lett. **B277** (1992) 183; **B283** (1992) 403; R.M. Barnett, R. Cruz, J.F. Gunion and B. Hubbard, Phys. Rev. **D47** (1993) 1048; V. Barger, R.J.N. Phillips and D.P. Roy, Phys. Lett. **B324** (1994) 236; J.F. Gunion, Phys. Lett. **B322** (1994) 125; and references therein.
- [6] H. Baer, M. Bisset, C. Kao and X. Tata, Phys. Rev. **D46**, 1067 (1992).
- [7] V. Barger, M. Berger, A. Stange and R. Phillips, Phys. Rev. **D45** (1992) 4128.
- [8] J. Gunion, R. Bork, H. Haber and A. Seiden, Phys. Rev. **D46**, 2040 (1992); J. Gunion, H. Haber and C. Kao, Phys. Rev. **D46**, 2907 (1992).

- [9] J.F. Gunion and L. Orr, Phys. Rev. **D46** (1992) 2052; J.F. Gunion, in *Perspectives on Higgs Physics*, ed. G. Kane, World Scientific Publishing (1992), and references therein.
- [10] Z. Kunszt and F. Zwirner, Nucl. Phys. **B385** (1992) 3.
- [11] G. Unal, D. Cavalli, L. Gozzi and L. Perini, EAGLE Internal Note, PHYS-NO-005 (1992).
- [12] CMS Technical Proposal, CERN/LHCC 94-38 (1994).
- [13] T. Garavaglia, W. Kwong and D.-D. Wu, Phys. Rev. **D48**, 1899 (1993).
- [14] J. Dai, J. F. Gunion and R. Vega, Phys. Lett. **B315** (1993) 355; Phys. Lett. **B345** (1995) 29.
- [15] A. Stange, W. Marciano, and S. Willenbrock, Phys. Rev. **D49** (1994) 1354; Phys. Rev. **D50** (1994) 4491.
- [16] H. Baer, D. Dicus, M. Drees and X. Tata, Phys. Rev. **D36** (1987) 1363.
- [17] K. Griest and H. Haber, Phys. Rev. **D37** (1988) 719.
- [18] A.S. Joshipura and S.D. Rindani, Phys. Rev. Lett. **69** (1992) 3269.
- [19] D. Choudhury and D.P. Roy, Phys. Lett. **B322** (1994) 368.
- [20] S.G. Frederiksen, N. Johnson, G. Kane and J. Reid, Phys. Rev. **D50** (1994) 4244.
- [21] J.F. Gunion, Phys. Rev. Lett. **72** (1994) 199.
- [22] H. Baer, M. Bisset, D. Dicus, C. Kao and X. Tata, Phys. Rev. **D47** (1993) 1062; H. Baer, M. Bisset, C. Kao and X. Tata, Phys. Rev. **D50** (1994) 316.

- [23] J. Botts *et. al.* Phys. Lett. **B304**, (1993) 159.
- [24] Y. Okada, M. Yamaguchi and T. Yanagida, Phys. Lett. **262B**, (1991) 54; Prog. Theor. Phys. **85**, (1991) 1.
- [25] J. Ellis, G. Ridolfi and F. Zwirner, Phys. Lett. **257B**, (1991) 83.
- [26] H.E. Haber and R. Hempfling, Phys. Rev. Lett. **66**, 1815 (1991); H.E. Haber, in *Perspectives on Higgs Physics*, ed. G.L. Kane, World Scientific, Singapore, (1992), and references therein.
- [27] H. M. Georgi, S. L. Glashow, M. E. Machacek and D. V. Nanopoulos, Phys. Rev. Lett. **40** (1978) 692.
- [28] R. Cahn and S. Dawson, Phys. Lett. **B136** (1984) 196.
- [29] M. Chanowitz and M. K. Gaillard, Phys. Lett. **B142** (1984) 85; Nucl. Phys. **B261** (1985) 379.
- [30] G. L. Kane, W. Repko and W. Rolnick, Phys. Lett. **B148** (1984) 367.
- [31] D. Dicus and S. Willenbrock, Phys. Rev. **D39**, (1989) 751.
- [32] R. Ellis, I. Hinchliffe, M. Soldate and J. van der Bij, Nucl. Phys. **B297** (1988) 221.
- [33] U. Baur and E. W. N. Glover, Nucl. Phys. **B339** (1990) 38.
- [34] C. Kao, Phys. Lett. **B328** (1994) 420.
- [35] E. Braaten, J.P. Leveille, Phys. Rev. **D22** (1980) 715.
- [36] M. Drees and K. Hikasa, Phys. Lett. **B240**, (1990) 455; (E)-*ibid.* **B262**, (1991) 497.
- [37] N. Brown, Z. Phys. **C49** (1991) 657.

- [38] We are grateful to Mike Bisset and Xerxes Tata for providing a computer program to check branching ratios for the MSSM Higgs bosons with SUSY particle decays.
- [39] T. Sjöstrand, *Computer Physics Commun.* 39 (1986) 347; CERN-TH.7112/93;
T. Sjöstrand and M. Bengtsson, *Computer Physics Commun.* 43 (1987) 367;
H. U. Bengtsson and T. Sjöstrand, *Computer Physics Commun.* 46 (1987) 43.
- [40] E. Barberio, B. van Eijk and Z. Was, CERN report, CERN-TH-5 (1990).
- [41] T. Sjöstrand, private communication.
- [42] We are indebted to Z. Kunszt and F. Zwirner for providing the computer program RADCORR.
- [43] S. Abdullin, A. Khanov, N. Stepanov, CMS TN/94-180 (1994).
- [44] R. Brun *et al.*, GEANT3, CERN DD/EE/84-1 (1986).
- [45] N. Stepanov, CMS TN/94-182 (1994).

Figures

FIG. 1 The total cross section of $pp \rightarrow \phi \rightarrow \mu\bar{\mu} + X$ in fb, as a function of M_A , with $\sqrt{s} = 14$ TeV, $m_t = 175$ GeV, $m_{\tilde{q}} = \mu = 1000$ GeV, and $\tan\beta = 1, 3, 10,$ and 30 , for (a) the H , (b) the h and (c) the A . The cross section of $pp \rightarrow H^0 \rightarrow \mu\bar{\mu} + X$ for the SM Higgs boson is also presented with $M_{H^0} = M_A$.

FIG. 2 The LHC discovery contours in the M_A versus $\tan\beta$ plane, for the H (solid), the h (dash) and the A (dot). Three cases are considered: (a) $L = 100 \text{ fb}^{-1}$, $\mu = m_{\tilde{q}} = 1000$ GeV, (b) $L = 100 \text{ fb}^{-1}$, $\mu = m_{\tilde{q}} = 300$ GeV, and (c) $L = 10 \text{ fb}^{-1}$, $\mu = m_{\tilde{q}} = 1000$ GeV. Other parameters are the same as in Fig. 1. The discovery regions are on the upper plane of the the parameter space.

FIG. 3 Invariant mass distribution ($d\sigma/dM_{\mu\bar{\mu}}$) of the background from (a) Drell-Yan, (b) W^+W^- , (c) $t\bar{t}$, and (d) $b\bar{b}$.

FIG. 4 The discovery contour in the M_A versus $\tan\beta$ plane, for the MSSM Higgs bosons via their muon pair decay mode, at $\sqrt{s} = 14$ TeV with an integrated luminosity of 100 fb^{-1} . This figure is generated from a simulation with the CMS performance and $m_{\tilde{q}} = \mu = 1000$ GeV. We have considered the total cross section of $pp \rightarrow \phi \rightarrow \mu\mu + X$, summed over the H , the h , and the A . The QED radiative corrections to background from the Drell-Yan process are included. The discovery region is on the upper plane of the the parameter space.

FIG. 5 Histograms of number of events as a function of $M_{\mu\bar{\mu}}$ for the signal and the background at $\sqrt{s} = 14$ TeV with $L = 100 \text{ fb}^{-1}$, $M_A = 80, 150$ GeV, and $\tan\beta = 30$. This figure is generated from a simulation with the CMS performance and $m_{\tilde{q}} = \mu = 1000$ GeV.

This figure "fig1-1.png" is available in "png" format from:

<http://arxiv.org/ps/hep-ph/9503415v1>

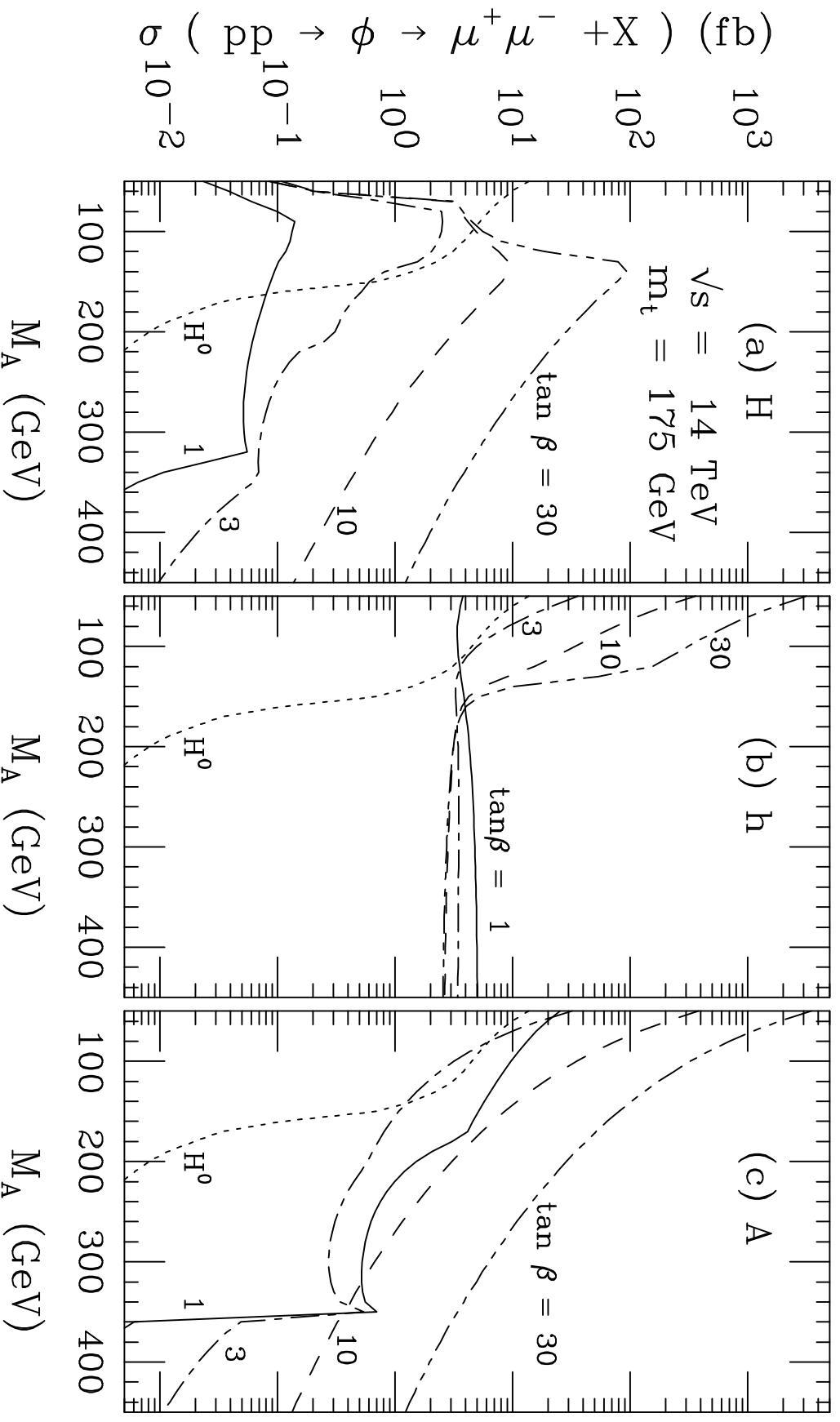


FIG 1/Kao and Stepanov

This figure "fig1-2.png" is available in "png" format from:

<http://arxiv.org/ps/hep-ph/9503415v1>

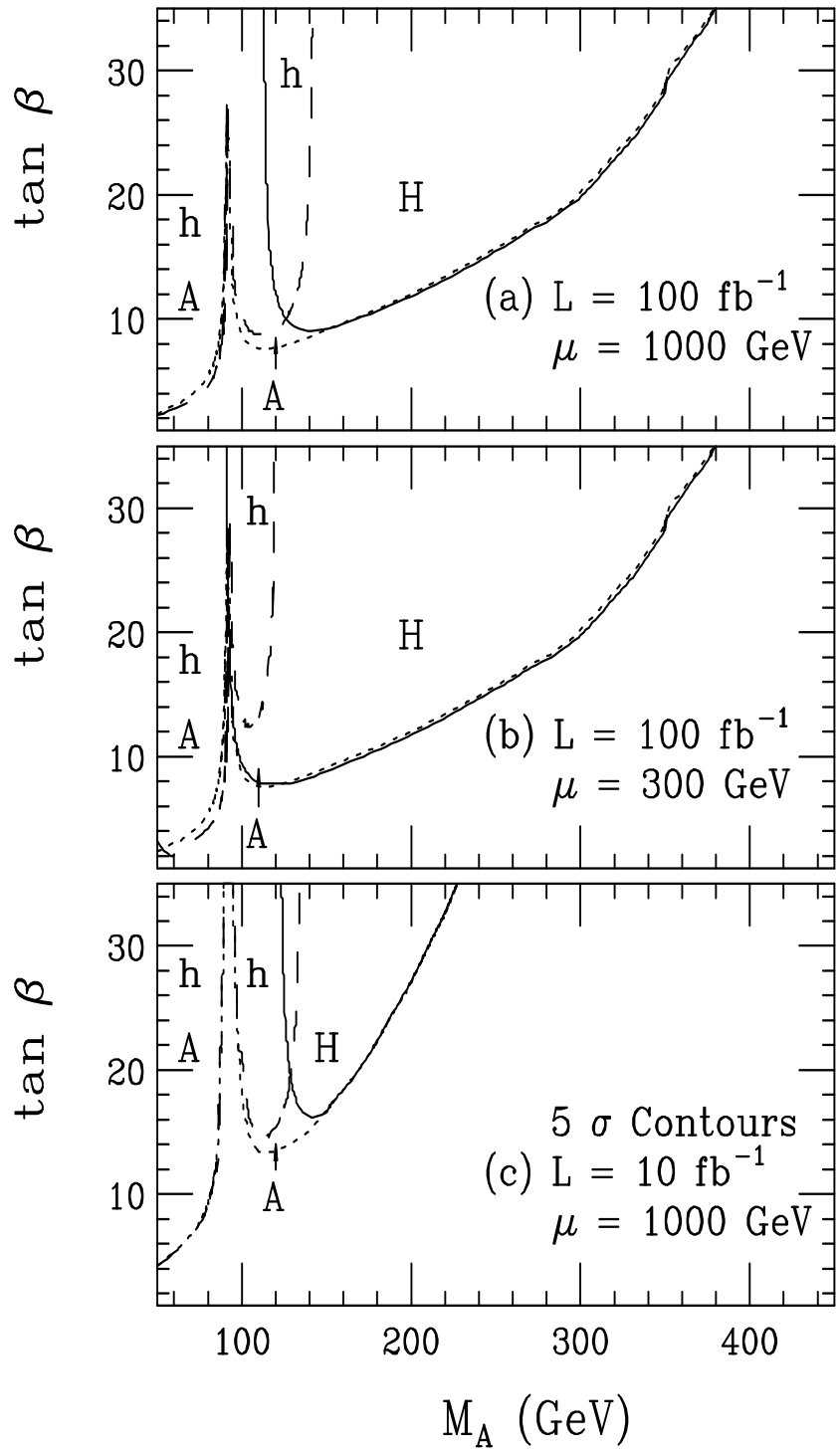


FIG 2/Kao and Stepanov

This figure "fig1-3.png" is available in "png" format from:

<http://arxiv.org/ps/hep-ph/9503415v1>

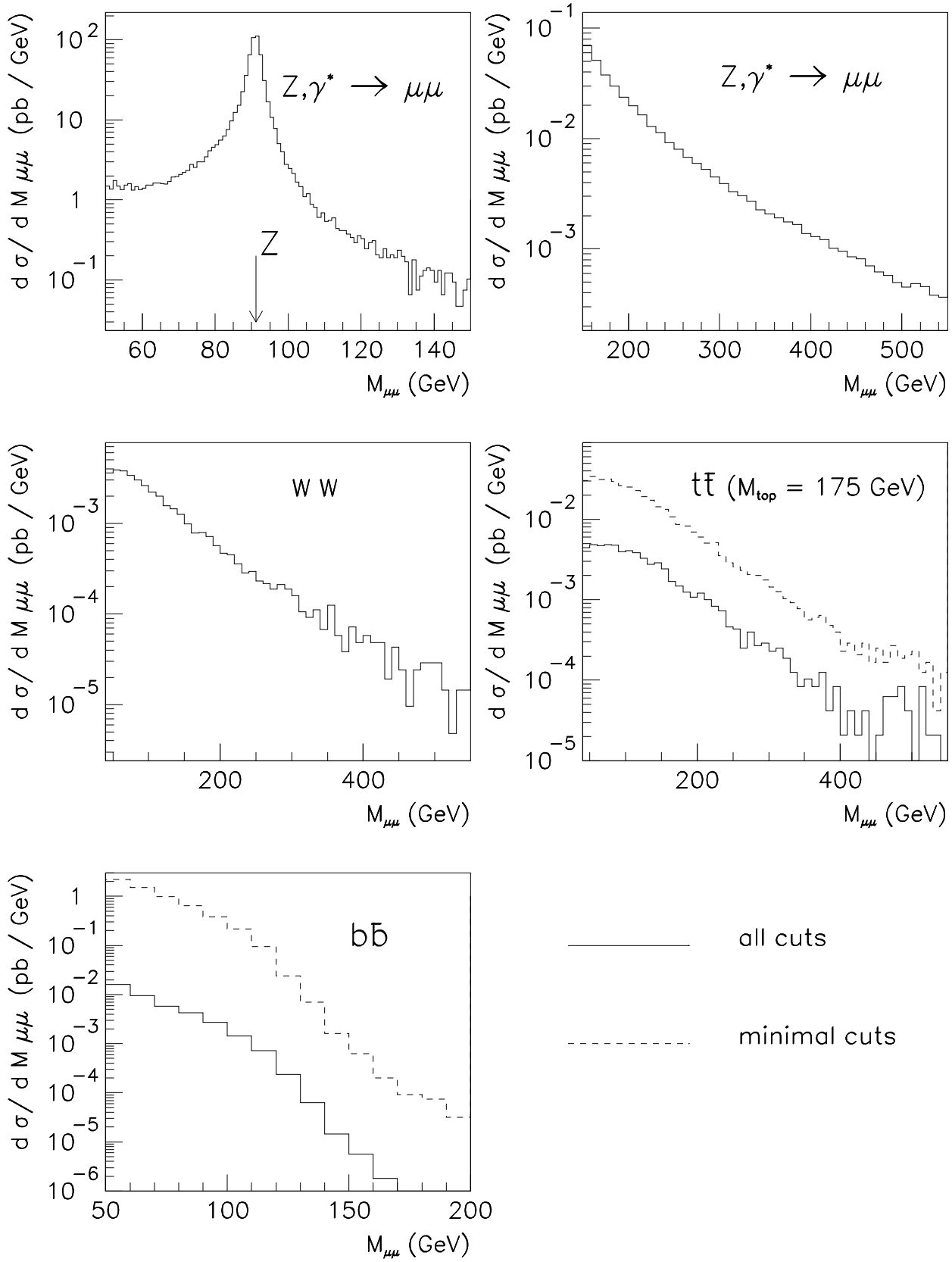


FIG 3/Kao and Stepanov

This figure "fig1-4.png" is available in "png" format from:

<http://arxiv.org/ps/hep-ph/9503415v1>

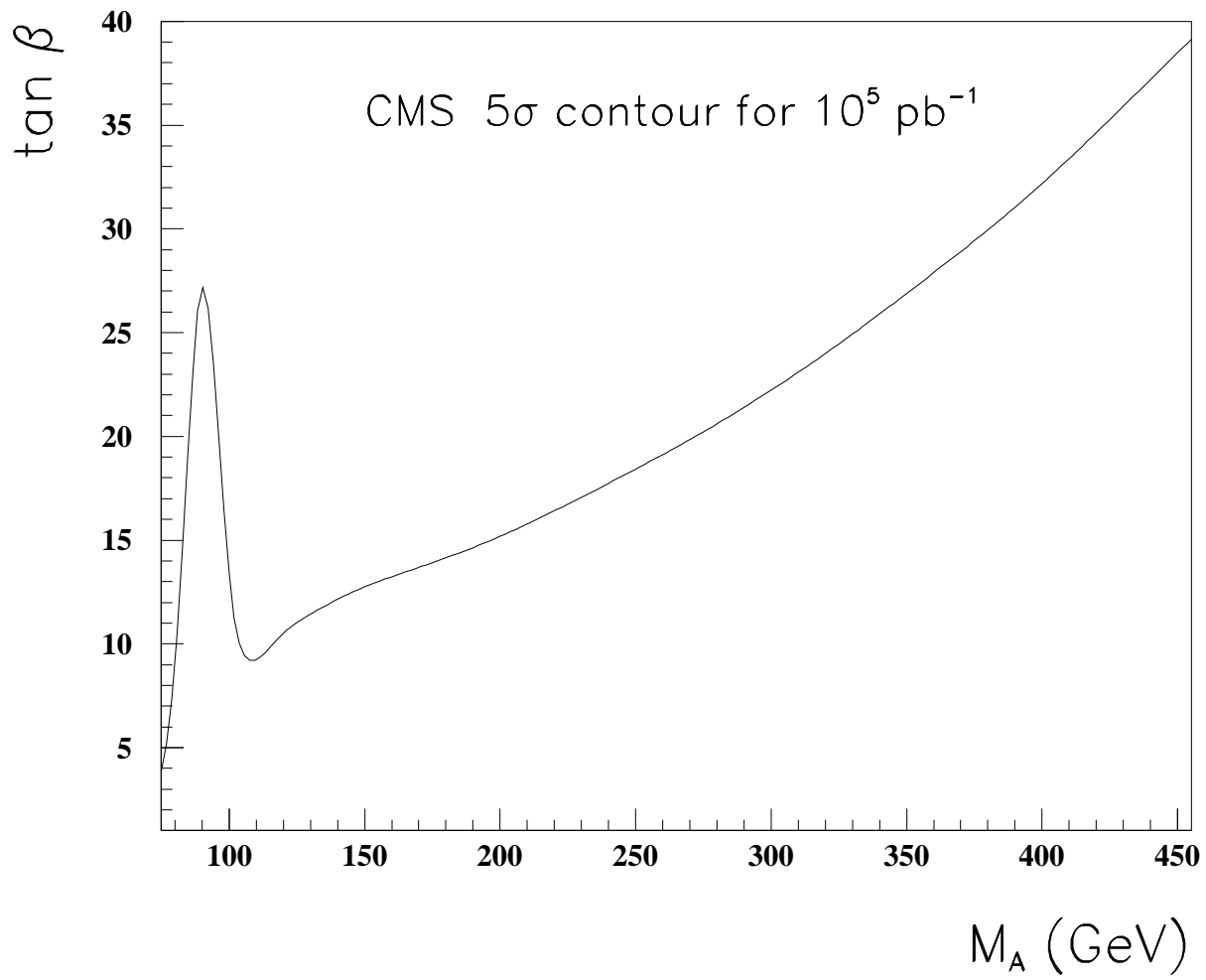
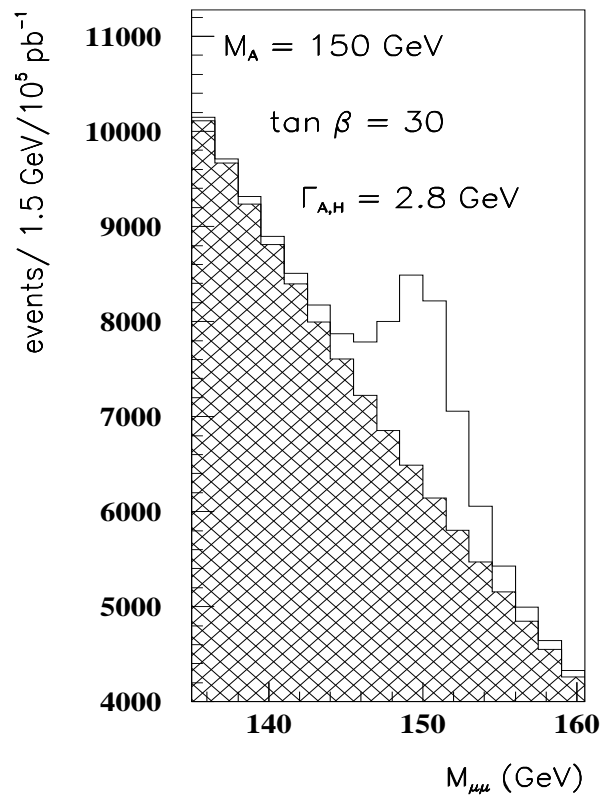
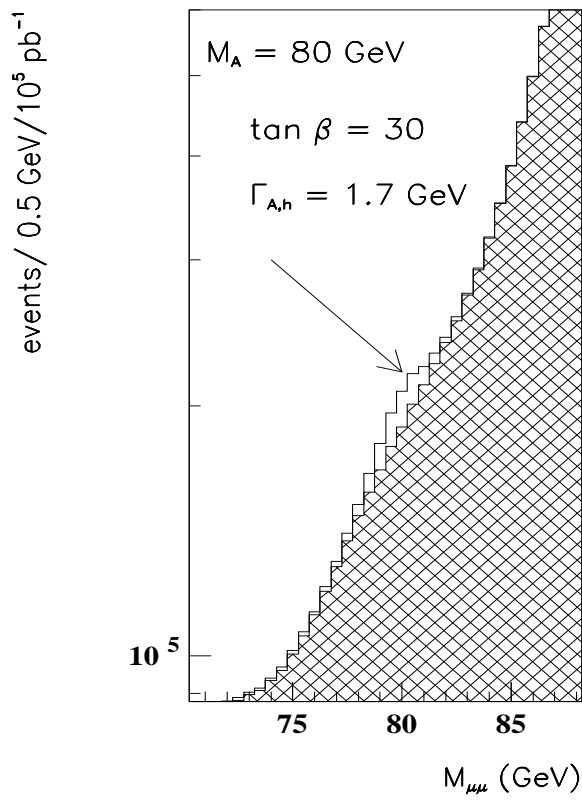


FIG 4/Kao and Stepanov

This figure "fig1-5.png" is available in "png" format from:

<http://arxiv.org/ps/hep-ph/9503415v1>



Smooth part of background is subtracted

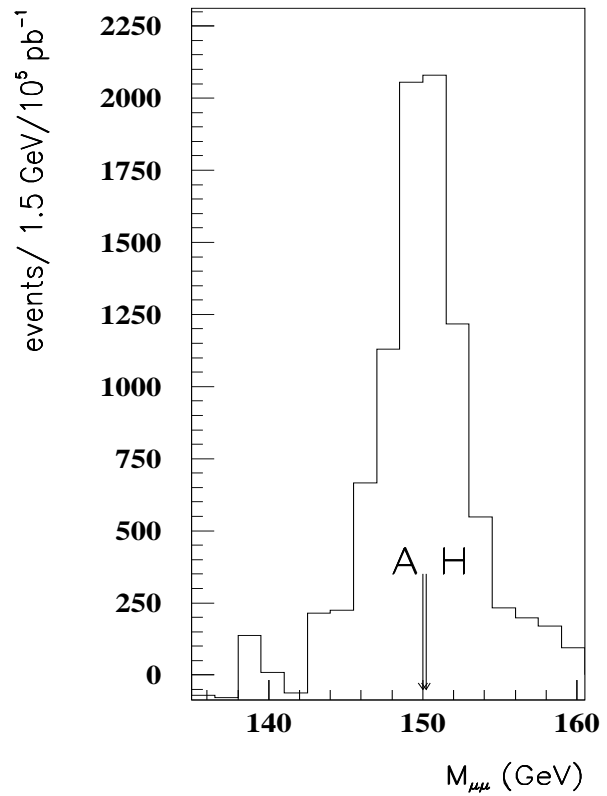
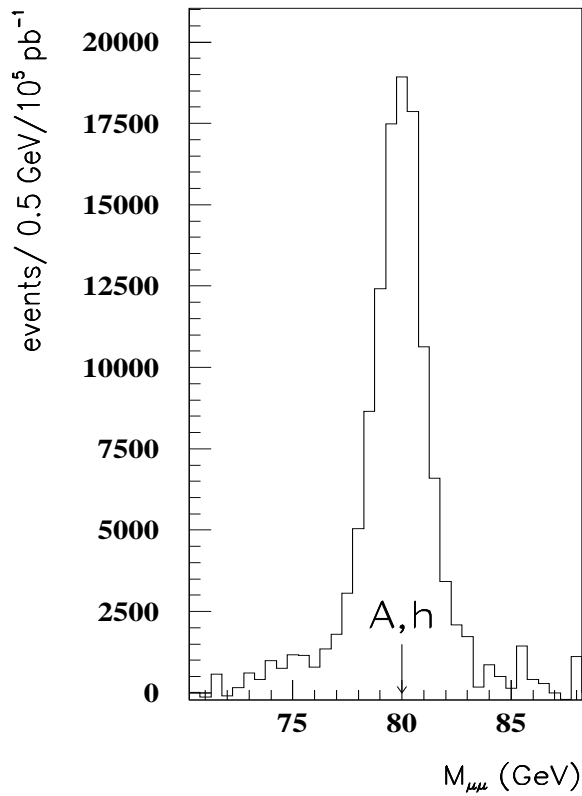


FIG 5/Kao and Stepanov